The Effect of Volcanic Eruptions on the Life Cycle of the Indian Summer Monsoon

A thesis
Submitted towards the partial fullfilment of
BS-MS dual degree programme
by

SHREYAS S IYER

DATE: 27/03/2025

under the guidance of

CLAUDIA TIMMRECK

MAX PLANCK INSTITUTE FOR METEOROLOGY

from May 2024 to Mar 2025

INDIAN INSTITUTE OF SCIENCE EDUCATION AND RESEARCH PUNE

Certificate

This is to certify that this dissertation entitled ”The Effect of Volcanic Eruptions on the Life Cycle of the Indian Summer Monsoon” submitted towards the partial fulfilment of the BS-MS degree at the Indian Institute of Science Education and Research, Pune, represents original research carried out by Shreyas S Iyer at Max Planck Institute For Meteorology, under the supervision of Claudia Timmreck during academic year May 2024 to Mar 2025.

Supervisor:
CLAUDIA TIMMRECK
GROUP LEADER
MAX PLANCK
INSTITUTE FOR
METEOROLOGY

Expert:
JOY MONTEIRO
ASSISTANT
PROFESSOR
IISER PUNE

DATE: 27/03/2025

Declaration

I, hereby declare that the matter embodied in the report titled ”The Effect of Volcanic Eruptions on the Life Cycle of the Indian Summer Monsoon” is the results of the investigations carried out by me at the ”Max Planck Institute For Meteorology” from the period 15-05-2024 to 15-03-2025 under the supervision of Claudia Timmreck and the same has not been submitted elsewhere for any other degree.

Supervisor:

CLAUDIA TIMMRECK

GROUP LEADER

MAX PLANCK

INSTITUTE FOR

METEOROLOGY

Student:

SHREYAS S IYER

20201010

BS-MS

IISER PUNE

DATE: 27/03/2025

Acknowledgements

Firstly, I would like to thank all of the collaborators of this project: my supervisor Claudia Timmreck, Moritz Günther, and Chetankumar Jalihal. I would also like to thank everyone who discussed this project with me. Hauke Schmidt, Ulrike Niemeier, Roberta D'Agostino, Bjorn Stevens, David Battisti, and the project expert Joy Monteiro all had valuable advice and inputs to give.

I want to acknowledge the funding received during my thesis from the Department of Science and Technology of the Government of India for the KVPY / INSPIRE fellowship and from the Max Planck Institute for Meteorology.

On a more personal note, the wonderful people I met in the uncharacteristically sunny city of Hamburg deserve a mention. My stay here would definitely not have been the same without the hours I spent walking, cycling and playing football with all of you. Also, to the numerous groups of urban apes who found me: you made the last few months pass by so quickly. I will miss staring at rocks with you.

Lastly, I would like to thank my family for their support and encouragement—and for going *above* and *beyond* to ensure I never felt too distant.

Abstract

Large volcanic eruptions are a source of climate variability, affecting global temperatures and precipitation. The hydrology of the Indian monsoon region is particularly sensitive to volcanic forcing. Previous studies have focused on the seasonal mean response of the Indian summer monsoon to eruptions. Here, we investigate changes in the onset and withdrawal of the monsoon, which are important characteristics that affect the water budget of the region. Using large ensemble simulations in the Max Planck Institute Earth System Model, with idealised eruptions that inject 40 Tg of sulphur into the stratosphere at varying latitudes, we find changes in the monsoon onset and withdrawal dates by a few weeks compared to an unforced case. We explain the changes in onset dates within the low-level jet and ITCZ frameworks, which have been used to explain the internal variability of the monsoon onset. We find that the length of the Indian summer monsoon is strongly dependent on the eruption latitude. Our results show a shorter (longer) Indian monsoon duration, as opposed to weakened (strengthened) monsoon circulation, drives changes in the total seasonal precipitation following a Northern (Southern) Hemispheric eruption.

Contents

List of Figures

Chapter 1

Introduction

Volcanic eruptions have an impact on the global climate. They affect precipitation patterns, particularly in the tropics, such as the monsoon. In this thesis, we investigate how volcanic eruptions impact the Indian monsoon. This introduction first provides an overview of volcanic eruptions and their effects on the climate. It is then followed by a section on the current understanding of the monsoons.

1.1 Volcanic Impact on Climate

1.1.1 Overview

Large volcanic eruptions inject sulphur-containing gases into the Earth's stratosphere. These gases oxidise to form sulphuric acid vapours, which condense and nucleate to form stratospheric sulphate aerosols. Owing to their low sedimentation velocity, stratospheric sulphate aerosols remain in the stratosphere for a few years [1]. Strong zonal winds in the stratosphere create a uniform zonal distribution of aerosols [2]. The vertical and meridional transport of the aerosols is determined by the Brewer-Dobson circulation (BDC), which transports aerosols poleward, from where they settle out of the stratosphere [3].

Stratospheric sulphate aerosols affect the energy budget of the Earth's atmosphere. Due to their high albedo, their primary effect is surface cooling caused by the scattering incident shortwave radiation. They also absorb longwave radiation from the surface, which increases the stratospheric temperature. Thus, the radiative effect of volcanic eruptions is to cool the Earth's surface and troposphere while warming the stratosphere. This causes changes to the stability of the atmosphere, affecting global circulation patterns, which in turn affects the hydrological cycle of the Earth [4]. Both the cooler troposphere and surface contribute to a reduction in precipitation. A cooler atmosphere experiences lesser condensation and precipitation, owing to its radiative

cooling [5]. Additionally, a cooler surface leads to the stabilisation of the atmosphere and a reduction in evaporation [6].

1.1.2 Impact on Precipitation

The impact of volcanoes on precipitation has been extensively studied in both proxy studies as well as models. Model studies, such as Broccoli et al. [7], found, in an ensemble framework, a reduction in terrestrial precipitation following a simulation of the Mt. Pinatubo eruption. Similar findings were made by Robock and Liu [8], who noted a significant reduction in global precipitation for 2-3 years following an eruption. In their study, tropical regions show the largest reduction in precipitation. This occurs in the maximum rainfall region, which is associated with the cooling and consequent weakening of the inter-tropical convergence zone (ITCZ).

The response of the ITCZ, as an important feature of tropical precipitation, to volcanic forcings has been investigated. Schneider et al. [9] suggested that the seasonal migration of the ITCZ into the summer hemisphere is restricted by volcanic eruptions, which was attributed to greater relative cooling of the summer hemisphere compared to the winter hemisphere. Studies such as Broccoli et al. [10] and Kang et al. [11] showed that hemispherically asymmetrical heating/cooling causes a displacement of the ITCZ towards the warmer hemisphere. Changes in the location and symmetry of the forcing, therefore, can vary the tropical precipitation response. Haywood et al. [12] and Zhuo et al. [13] show that a Northern (Southern) hemispheric eruption displaces the ITCZ to the South (North).

The monsoons are another important feature of tropical precipitation affected by volcanic forcings. Schneider et al. [9] found large decreases in precipitation over the summer monsoon regions, with a zonal precipitation reduction on the order of 15%. Monsoon rainfall patterns are also sensitive to the location of volcanic forcings. Zhuo et al. [14] and Liu et al. [15] using model studies, as well as Zuo et al. [16] using paleo proxies, show that the monsoon precipitation reduces (increases) when there is an eruption in the same hemisphere but decreases (increases) when the eruption occurs in the opposite hemisphere, attributed to changes in the strength of the monsoon circulation. However, they disagree on the Indian summer monsoon's response to tropical eruptions, with Zhuo et al. [14] finding an increase in precipitation, while the latter two find a decrease. The latter result is in agreement with D'Agostino and Timmreck [17], who find that tropical eruptions reduce the monsoon intensity in the Northern Hemisphere. Despite the symmetrical forcing, zonally asymmetric anomalies in rainfall in the monsoon regions occur. Additionally, they found that the strength of monsoon precipitation reduction is correlated with eruption strength, but significant decreases in monsoon precipitation do not occur below a threshold of eruption strength.

Proxy studies, including Tejedor et al. [18], also find a hemispherically asymmetric response to volcanic eruptions, with latitudes North of the equator drying, and the Southern hemisphere wettening. However, over the Indian monsoon region, Anchukaitis et al. [19] highlights the disagreement on the hydrological response between global circulation models and proxy data, with the latter showing wetter conditions.

1.2 Monsoons

To understand the impact of volcanoes on monsoon precipitation, we first review the current understanding of the monsoons. Monsoons are seasonal reversals of upper- and lower-level winds, associated with the rainy season in many tropical and subtropical latitudes. In this thesis, we look at the volcanic impact on the strongest regional monsoon, the Indian Summer Monsoon (ISM) [20].

The monsoon season is responsible for most rainfall that occurs over a large portion of the Indian region, so the total yearly water budget is strongly dependent on the ISM [21] and is affected by the internal variability of the monsoon [22]. The duration of the monsoon season, bound by the onset and demise of the ISM, is also correlated with the total monsoon rainfall [23]. Moreover, variations in the life cycle of the ISM are of economic relevance, being critical to the region's agricultural output [24, 25]. Therefore, as important aspects of the ISM, we are interested in the response of the onset, demise, and length of the monsoon to volcanic forcings. It is thus important to discuss the existing frameworks used to understand the monsoon's life cycle.

1.2.1 Monsoon Frameworks

Although the ISM was previously understood as a continental-scale sea breeze driven by the summer heating of the subcontinent, it is now understood to be a regional, poleward extension of the ITCZ [26]. Bordoni and Schneider [27] showed that the meridional overturning circulation in the Asian monsoon region rearranges itself during monsoon onset, from a near-hemispherically-symmetric 'equinox' pattern to a 'monsoon' pattern, with a large cross-equatorial cell that ascends in the subtropics of the summer hemisphere. This rearrangement in tropical circulation brings with it changes in the location of the tropical rain-belt, or the ITCZ. However, the term 'ITCZ' is problematic over the Indian summer monsoon latitudes due to the presence of two maximum cloud zones [26]. Therefore, we will use the term 'tropical convergence zone' (TCZ) to refer to the tropical rain-belt region. This movement of the TCZ is thus important in determining the transition between these two patterns and the life cycle of the ISM.

Although the transition between the equinox and monsoon patterns was found to

occur even in the absence of meridional land-sea temperature contrasts [27], the monsoon onset is influenced by surrounding topography [21] and land-sea temperature contrasts [28]. In the Indian monsoon region, the presence of the TCZ in the Northern hemisphere establishes cross-equatorial winds. These winds are confined over a narrow region in the Arabian Sea, known as the Somali (or low-level) jet (LLJ) [29]. The onset of ISM is caused by increased surface wind convergence and upward moisture flux. This, in turn, is attributed to the strengthening of the LLJ, which, when decelerating over the Indian subcontinent, leads to an increased wind convergence. [30].

A stronger and more Northerly low-level jet in the premonsoon months has been associated with an earlier onset of the monsoon, which Chakraborty and Agrawal [31] have explained using a 'West Asian' heat low framework. They investigate interannual differences in onset dates over India and find that surface pressure anomalies over the region immediately West of India drive variations in the onset dates of the ISM. They suggest that differential heating of land and sea over the region west of India (what they refer to as West Asia) creates a pressure gradient that strengthens the LLJ. A weakening of this pressure gradient is observed in years with late onset and is accompanied by a weaker LLJ. In their study, surface pressure differences leading to shifted onset dates are seen months before the actual onset date.

1.3 The research question

Studies of the ISM, including those studying their response to volcanoes, use a fixed calendar period, often the months of June to September (although the inclusion of May or the exclusion of September also occurs). This is also reported by Bombardi et al. [32], who, in their review of monsoon timing, mention that most published reports of the ISM use a fixed seasonal mean. Although this is the climatological rainy season, results can be contaminated by the inclusion of dry season data.

This seasonal mean picture has been used to understand the impact of volcanic eruptions on the monsoon. The current understanding is that volcanic eruptions reduce the total seasonal precipitation by weakening the monsoon circulation and reducing the intensity of monsoon rainfall, which has been attributed to changing land-sea temperature differences.

However, we also know the following:

- Volcanic eruptions displace the TCZ [12], affecting the transition from the equinox to the monsoon regime [27], which could affect the length of the monsoon season.
- The length of the monsoon season is correlated with the total monsoon rainfall [23]

Consequently, when determining the impact of volcanoes on the ISM, it is important to investigate changes not only to the seasonal mean but also to its timing and duration. Since the impact of volcanic eruptions on the life cycle of the monsoon has not been studied previously, it remains unclear to what extent the changes in either the monsoon duration or the monsoon intensity are responsible for the changes in monsoon precipitation. In this thesis, using the global coupled general circulation model MPI-ESM1.1, we ask the following:

- How do the ISM's life cycle characteristics, which are its onset, demise and length, respond to volcanic eruptions?
- How do these responses integrate within the ITCZ and LLJ frameworks that are used to understand the monsoon and its onset?
- What role is played by the monsoon season length in determining the sensitivity of monsoon precipitation to volcanic eruptions?

Chapter 2

Data and Methods

2.1 Why Models?

The internal variability of the ISM makes it difficult to ascertain the effect of a single volcanic eruption. Only a few large eruptions exist in recorded history, so proxy reconstructions of historical data have been used to study the climate impact of volcanoes [33]. However, historical eruptions vary not just in eruption magnitude but in location and season as well, which makes it challenging to understand the effects of any one of these factors.

Simulated volcanic eruptions in climate models allow us to remove these variations and study the effects of changing one factor. Climate models can also be used to generate large ensembles, which facilitate the separation of internal variability from external forcings [34]. Differences in the internal variability of the monsoon are averaged out with a sufficiently large ensemble. The resulting ensemble-mean signal contains the signal of the external volcanic forcing. 100-member ensembles are large enough to detect the temperature changes following a volcanic eruption, both at a global [34] and a regional scale [35]. In this study, we use the EVA-Ens model [36], which is a 100-member ensemble based on the Max Planck Institute Earth System Model (MPI-ESM) [37]. EVA-Ens branches off historical simulations of the Max Planck Institute Grand Ensemble (MPI-GE [38]) in January 1991. The MPI-GE consists of 100-member ensembles based on the low-resolution version of the Max Planck Institute Earth System Model (MPI-ESM1.1-LR). In the MPI-ESM1.1-LR, the atmospheric general circulation model ECHAM6.3, with a horizontal resolution of 200km and 47 vertical levels up to 0.01 hPa [39] is coupled with the ocean sea-ice model MPIOM, with 1.5° ocean resolution and 64 vertical levels [40].

The MPI-ESM has been used successfully to determine the climate response to volcanic eruptions (eg. D'Agostino and Timmreck [17], Azoulay et al. [36], Zhuo et al. [14]. It has shown agreement with other low-resolution CMIP6 models in intermodal

comparison studies with regard to global surface climate responses [41]. MPI-ESM simulations of the Pinatubo eruption also show agreement with observed data [42].

2.1.1 Comparison With Observational Data

Nevertheless, we test the ability of the MPI-ESM to represent the monsoon by comparing it with observed precipitation data from the Indian Meteorological Department (IMD). 72 years of daily gridded data (1952 to 2024) at a horizontal spatial resolution of 1° is used [43]. The IMD data was downloaded using the python library *imdlib* [44].

2.2 EVA-Ens

The effects of volcanic eruptions on the global climate are simulated by prescribing different forcing fields of volcanic aerosols. The prescribed forcing for the June 1991 Pinatubo eruption is replaced with idealised fields calculated using the Easy Volcanic Aerosol (EVA) forcing generator [42]. The EVA generator calculates aerosol forcing as fields of single scattering albedo (SSA), wavelength-dependent aerosol extinction (EXT) and the asymmetry factor (ASY) as a function of volcanic sulphur emission, season, location and wavelength. These are passed as inputs into the radiative scheme of the EVA-Ens as monthly zonal mean wavelength-dependent optical properties.

The EVA forcing generator tries to balance realism (with respect to observation), with generality (being able to represent different eruptions consistently). Although it has a simple design, inaccuracies in its volcanic forcing properties are small compared to those derived from proxies. Rather than perfectly reproducing volcanic aerosols, it captures those properties that are relevant to the climate [42].

We analyse 100-member ensemble simulations of three eruptions varying in eruption latitudes. These are tropical **(TR)** and two extratropical: northern hemispheric **(NH)** and southern hemispheric **(SH)**. The experiments are run for a period of 5 years, from January 1991 to December 1995, with 6-hourly output. The prescribed forcing fields correspond to an eruption strength of 40 Tg of sulphur, which is an approximate mean of the estimated stratospheric sulphur emissions from the 6 strongest eruptions in the past 2500 years [45]. As a reference for the scale of the experimental eruptions, the Pinatubo eruption injected around 10 Tg of sulphur into the stratosphere [3]. Additionally, an unforced 100-member ensemble simulation is used as a control **(CO)**.

In Figure 2.1, we see the aerosol optical depth (AOD) forcing field prescribed to the model and its time evolution. Although an eruption occurs in June 1991 for all experiments, the subsequent movement of aerosols is determined by the latitude of the eruption. While the stratospheric aerosols in the **NH** and **SH** experiments remain

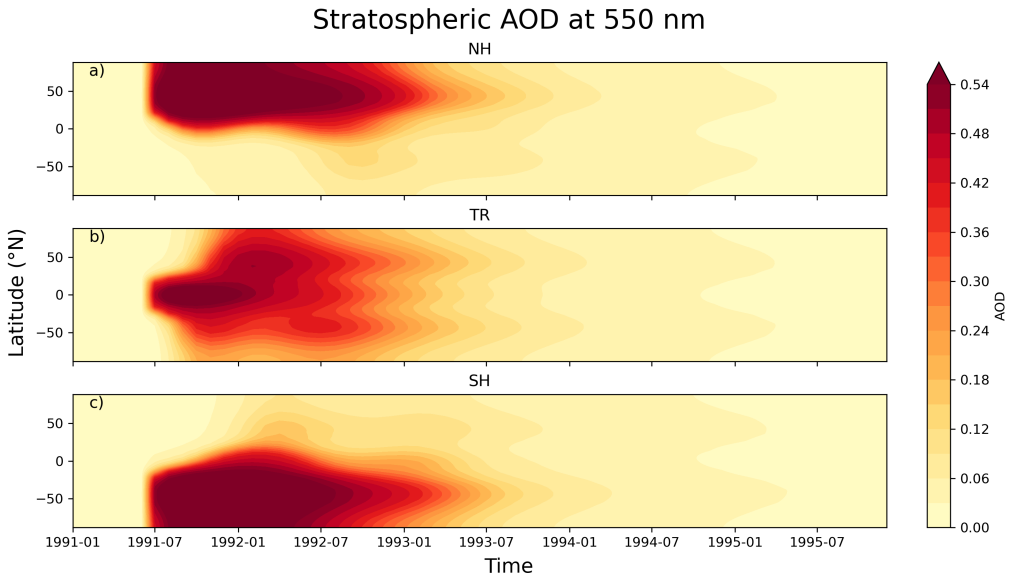

Figure 2.1: A Hovmöller plot of the zonal-mean stratospheric aerosol optical depth (AOD) at 550 nm for the three forced experiments a) **NH** b) **TR**, and c) **SH**, which differ in the latitude of volcanic forcing. The simulated volcanic eruption occurs in June 1991, seen as a large increase in stratospheric AOD.

largely confined to their respective eruption hemispheres, in the **TR** experiment, the aerosols are transported to both poles.

2.3 Defining Monsoon Onset and Demise

The onset of monsoon in India has multiple definitions [32]. These differing monsoon definitions exist to address different problems. A retrospective definition of monsoon cannot be used to predict onset, while a definition over the entire subcontinent is useful when considering large-scale circulation but can differ from the actual onset at a particular location by weeks. Additionally, multiple atmospheric variables can be used to mark the rainy season, including rain, outgoing longwave radiation (OLR), wind velocity, etc.

The onset of the ISM is often marked by onset over the south-west of the country. However, these dates are not well correlated with the total ISM rainfall. Monsoon onset defined over a central Indian region better represents rainfall over the entire region [31, 23].

Noska and Misra [23] defined the onset of the ISM using the daily precipitation anomaly with respect to a multi-decadal average climatology. The cumulated daily precipitation anomaly in a calendar year exhibits points of inflection during the start and end of the monsoon season. Based on spatially averaged rainfall, this defines the onset and withdrawal date over the entire region. Given spatially averaged rainfall

$R(d, y, e)$ on day d of calendar year y, and ensemble member e, we find the daily climatology $\overline{C}_y$.

$$\overline{C}_y = \frac{\sum_{d=1}^{D} \sum_{e=1}^{100} [R(d, y, e)]}{100D} \tag{2.1}$$

The cumulative precipitation anomaly $A_{d,y,e}$ on a calendar day d is:

$$A_{d,y,e} = \sum_{i=1}^{d} (R(i, y, e) - \overline{C}_y) \tag{2.2}$$

$$\vec{A}_{y,e} = [A_{0,y,e}\ ,\ \ A_{1,y,e}\ , \cdots A_{D,y,e}] \tag{2.3}$$

where D is the number of calendar days in year y.

The day after the minimum value of $\vec{A}_{y,e}$ is found is the onset day $O(y, e)$. In order to ensure that the demise day occurs after the onset, the maximum value of $\vec{A}_{y,e}$ is found only for days after $O(y, e)$, and demise $D(y, e)$ is defined as one day after this maximum value. These onset and demise dates are calculated for each year and ensemble member, while the length of the monsoon season is found from their difference.

$$O_{y,e} = \arg(\min_{d} \vec{A}_{y,e}) + 1 \tag{2.4}$$

$$D_{y,e} = \arg(\max_{d>O(y,e)} \vec{A}_{y,e}) + 1 \tag{2.5}$$

In this study, all monsoon characteristics are calculated over the central Indian region: $70 - 85$ °E, $15 - 25$ °N. The onset and demise are calculated using spatially averaged rainfall over this region. Although we use rainfall to define the onset and demise, this methodology is valid for any atmospheric variable that rapidly transitions between monsoon and non-monsoon periods. An example of the methodology is used in Figure 2.2 uses rainfall to exhibit two distinct 'rainy' and 'non-rainy' states and a fast transition between them.

We compare the onset and demise dates calculated using the same methodology with two variables: precipitation and OLR. However, the maximum and minimum of cumulative OLR anomalies correspond to onset and demise, respectively, since the OLR is lower in the monsoon than in non-monsoon periods.

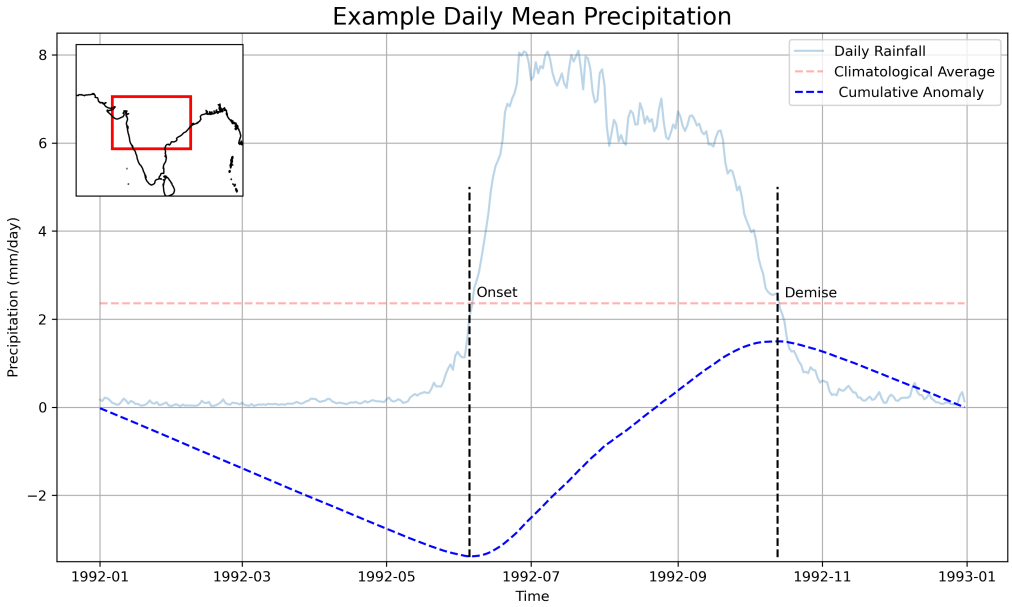

Figure 2.2: Ensemble-mean spatially averaged daily rainfall in the model year 1992, over central India ($70-85$ °E, $15-25$ °N) in the **CO** experiment is used. The onset and demise dates occur one day after the minimum and maximum, respectively, of the cumulative rainfall anomaly in a calendar year.

Although this methodology has various advantages:

1. Onset and demise are defined relative to the climatological rainfall, so they can be easily defined for monsoon regions with different intensities.
2. Usability on multiple scales, from local to regional onset and demise [46]
3. Flexibility in the choice of variable, allowing the comparison of onset and demise dates determined by different variables.

There is a known limitation of this methodology, which occurs when, throughout the year, the daily precipitation is below the climatological average. In this case, the cumulative anomaly monotonically decreases, which creates a trivial maximum and minimum at the beginning and end of the year, respectively. A solution to this involves normalizing the yearly rainfall by the total yearly precipitation. This preserves the relative contribution of each calendar day to the yearly rainfall and prevents trivial extrema from forming, which facilitates the calculation of onset and demise dates.

The normalized daily rainfall $N(d, y, e)$ is:

$$N(d, y, e) = \frac{R(d, y, e)}{\sum_{d=1}^{D}[R(d, y, e)]} \tag{2.6}$$

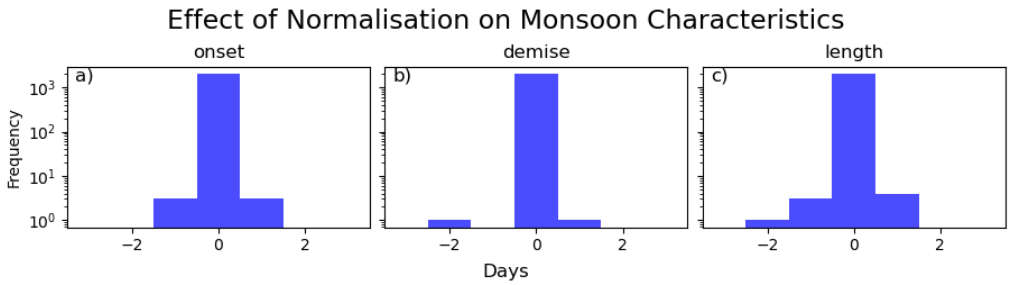

Figure 2.3: Histograms of the difference between unnormalised and normalised values of a) onset, b) demise and c) length, calculated using spatially averaged rainfall over central India.

We first used the methodology without normalisation. An analysis of the four model experiments and IMD data yielded no instances of poorly defined onset and demise dates when using a rainfall-based definition. However, when using an OLR-based definition, the onset and demise dates are poorly defined. The normalisation of daily OLR provides a better definition of the onset and demise dates in the forced experiments. However, the monsoon characteristics in our experiments are based on precipitation, which is largely unaffected by normalisation, which we see in Figure 2.3. Only a small fraction of the onset and demise dates are affected at all by normalisation, with all of them within 3 days from the unnormalised values. Therefore, we do not apply normalisation to the rainfall data. However, normalisation is still used on the OLR data to provide a comparison using different variables.

2.4 Moisture Flux

Monsoon onset follows the LLJ strengthening due to an increased convergence of moisture over the Indian subcontinent. Therefore, both the moisture carried by and the deceleration of the LLJ are important in determining the monsoon onset.

The moisture flux $F_{q,p}$ at a given pressure level p is:

$$F_{q,\,p} = \rho_p \; q_p \cdot \mathbf{v}_p \tag{2.7}$$

Where $\rho_p \; q_p$ and $\mathbf{v}_p$ are the density, specific humidity and horizontal velocity vector at pressure level p. From this, we find the column-integrated moisture flux:

$$F_q = \frac{1}{g} \int_{p_s}^{p_t} q \cdot \mathbf{v} \; dp \tag{2.8}$$

The above equation must be discretised, as the model provides variables at 47

pressure levels. We use 17 of these levels to get the discretised equation:

$$F_q \approx \frac{1}{g} \sum_{i=1}^{17} q_i \cdot \mathbf{v}_i \, \Delta p_i \tag{2.9}$$

Where Δp_i is found from the pressure levels as:

$$\Delta p_i = \frac{p_{i-1} + p_{i+1}}{2}, \quad 1 < i < 17 \tag{2.10}$$

$$\Delta p_1 = \frac{p_1 - p_2}{2} \tag{2.11}$$

$$\Delta p_{17} = \frac{p_{16} - p_{17}}{2} \tag{2.12}$$

The moisture flux convergence (MFC) over central India is then found as the sum of fluxes over its boundary.

$$\text{MFC} = \sum_{70^\circ\text{E}}^{85^\circ\text{E}} F_y\Big|_{15^\circ\text{N}} - F_y\Big|_{25^\circ\text{N}} \; + \sum_{15^\circ\text{N}}^{25^\circ\text{N}} F_y\Big|_{70^\circ\text{E}} - F_y\Big|_{85^\circ\text{E}} \tag{2.13}$$

Chapter 3

Results and Discussion

3.1 How Well is the Monsoon Represented?

First, we want to ensure that the core features of the monsoons are represented in the model, and whether the methodology used is reasonable.

So, in Figure 3.1, we compare the onset and demise dates of the ISM using both **CO** and IMD rainfall. Additionally, we compare these with an OLR-based definition of onset and demise. In each sub-figure, we find two white bands separating the monsoon and non-monsoon regions. These white bands indicate, at each latitude, that the variable has attained a climatological mean value, and are associated with the onset (on the left of the figure) and the demise (on the right of the figure). What we note from Figure 3.1 are:

- The normalised-OLR-based and precipitation-based definitions of monsoon onset and demise are in agreement with each other in the **CO** experiment
- The rainfall-based onset and demise are consistent between the **CO** experiment and the IMD data.
- The monsoon onset and demise don't occur simultaneously at all latitudes, as seen by the progression of the white bands. A Northward progression of monsoon onset, which is consistent with the observed monsoon, is present in the model using both rainfall and OLR-based definitions Figure 3.1. Similarly, the demise, although less sharp, has a clear Southward progression.

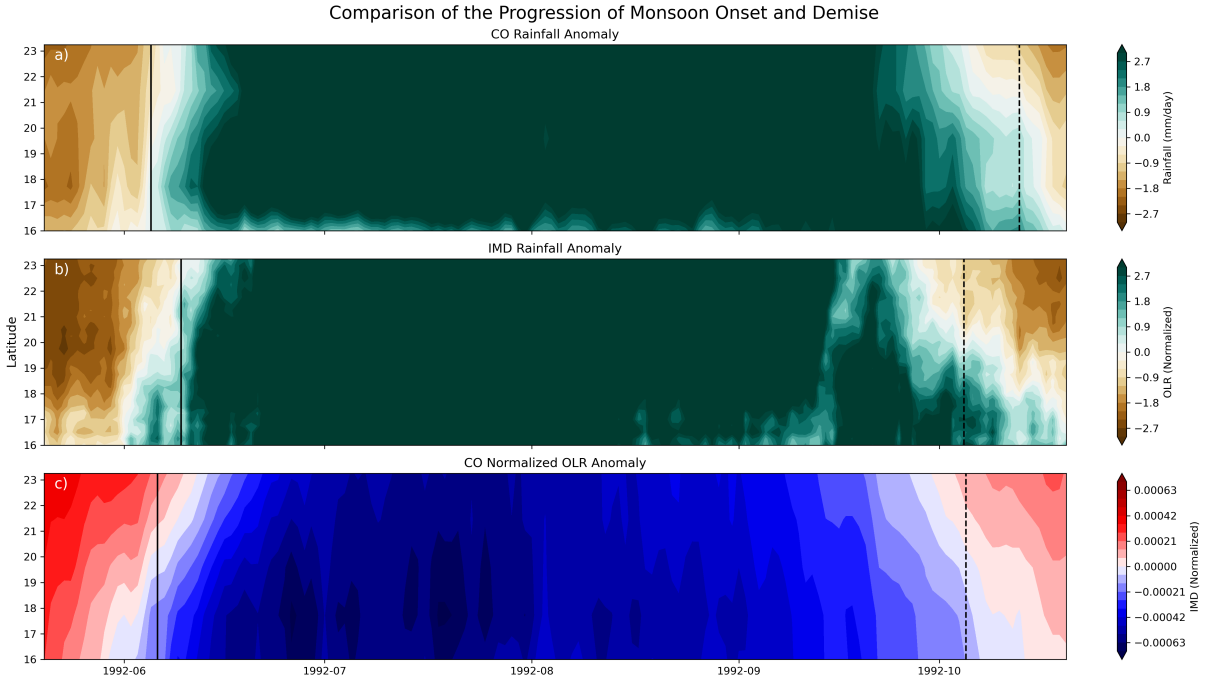

Figure 3.1: A Hovmöller plot of the 1992 monsoon season, The ensemble-mean anomaly of a) rainfall in the **CO** experiment, b) IMD's mean 1952-2024 rainfall and c) normalised OLR in the **CO** experiment are shown. The vertical solid lines indicate the date of onset over the region, while the vertical dotted lines indicate demise. In a) and b), brown shading indicates a below-climatological rainfall, while green shading indicates above-climatological rainfall. Similarly, in c), red shading indicates an above-climatological OLR, while blue shading indicates a below-climatological OLR.

Although we see that the model is consistent between different variables, and shows multiple features of the monsoon, we still compare the onset, demise and length of the monsoon with historical data. The monsoon in the unforced **CO** experiment exhibits variations between ensemble members solely due to its internal variability. Observational data of the past 72 years of monsoons also show internal variability. Thus, a comparison of these variations and their average monsoon characteristics helps determine the reliability of the model.

In order to ensure consistency, the same methodology and spatial region are used to calculate the monsoon characteristics in the IMD data. These results are in Figure 3.2, where we find a good agreement between the model and IMD data regarding monsoon characteristics. In addition, the different model years also show agreement among themselves.

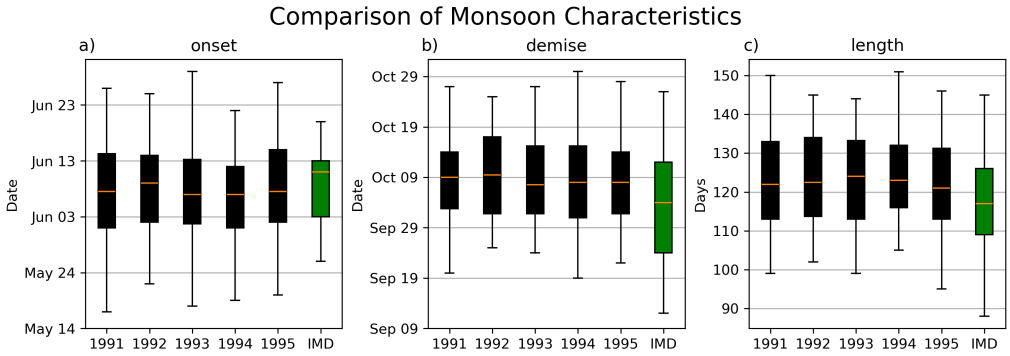

Figure 3.2: Monsoon onset, demise, and length calculated for daily gridded IMD data (in green) and separately for each year in the **CO** experiment (in black). For the IMD data, the spread is due to interannual variations, while in the **CO**, the spread is the ensemble-member variability. The boxes show the interquartile range of ensemble members, while the whiskers contain 95% of values around the median (orange line).

3.2 Monsoon Characteristics

We find that large volcanic eruptions cause a shift in both the onset and demise dates (and consequently the length) of the ISM. In Figure 3.3, we find shifted onset and demise dates in the three forced experiments when compared to **CO**. The **NH** experiment exhibits the largest variation in median onset and demise dates compared to **CO**. The median onset is delayed by 12 days, while the median demise is advanced by 19 days. The **TR** experiment also exhibits a delayed onset and advanced withdrawal, although with a smaller magnitude of difference compared to **NH**. The shift in monsoon characteristics in the **SH** experiment is opposite to the other experiments, with an 8-day advanced median onset and a 3-day delayed withdrawal. As a comparison, the standard deviation of the interannual variation of the onset date of the ISM over the central Indian region was shown by Chakraborty and Agrawal [31] to be 7 days.

The shifts in monsoon onset and demise are most prominent in the first two post-eruption years (1992 and 1993) when the concentration of stratospheric aerosols is the highest. In the final year of the experimental runs (1995), due to a reduced concentration of stratospheric aerosols, there is also a reduction in the magnitude of shifts in the monsoon onset, demise and length.

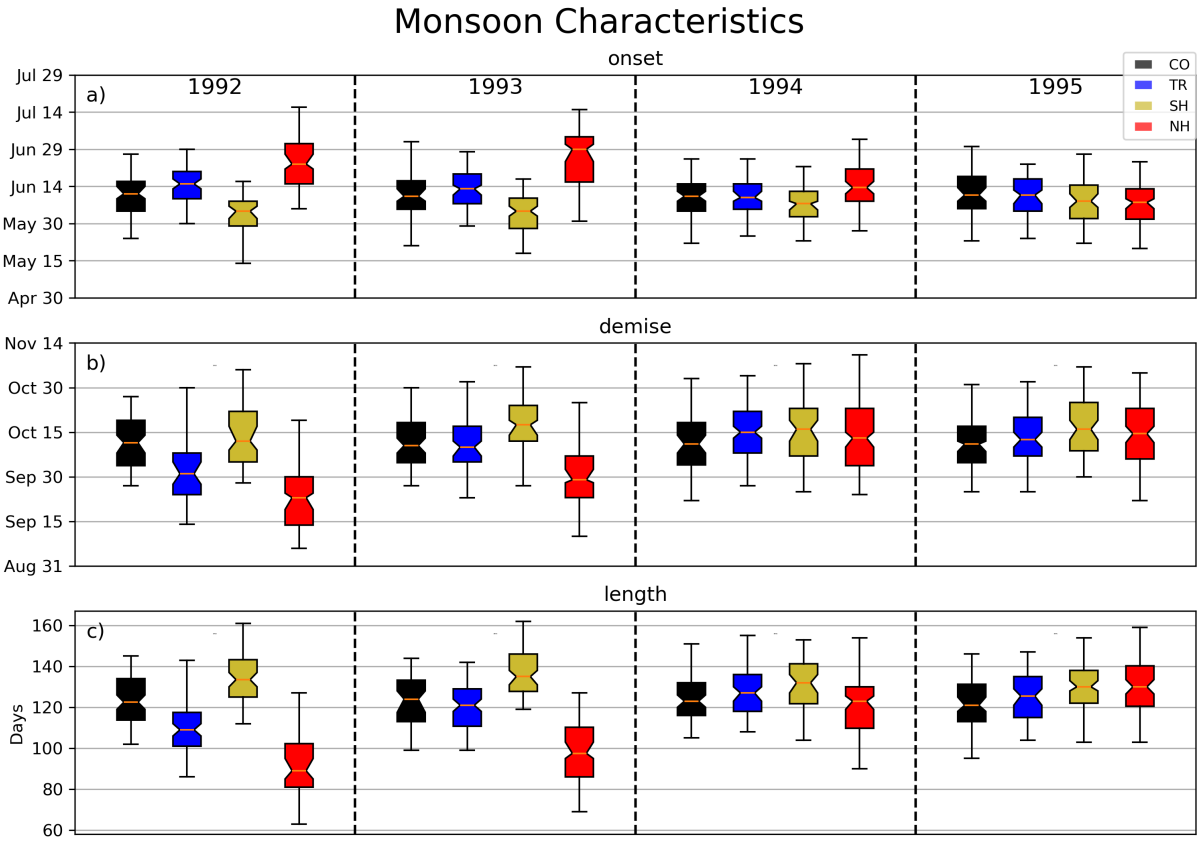

Figure 3.3: Variation of monsoon a) onset, b) demise and c) length for the model years 1992 - 1995. The boxes show the interquartile range of ensemble members, while the whiskers contain 95% of values around the median (orange line). Notches indicate the 95% confidence interval around the median generated by bootstrapping 50 (of the 100 members) with 10,000 resamples.

Since the onset and demise dates are shifted in opposite directions in the forced experiments, this results in large differences in the length of the monsoon season. In the model year 1992, compared to the median **CO** monsoon season, the monsoon duration in the **NH** experiment is roughly 27% shorter, while in **SH**, it is 9% longer.

3.2.1 Tropical Convergence Zone Framework

In order to understand why these shifts in monsoon timing and duration occur, we first analyse the results in the context of the TCZ transitioning between the equinox and monsoon patterns. A South-shifted TCZ (caused by a Northern hemispheric eruption) would switch from an equinox pattern to a monsoon pattern later in the boreal summer. This would result in a later ISM onset, and an earlier ISM withdrawal, which is in agreement with our results. We analyse the response of the TCZ to different volcanic forcings in Figure 3.4 to test this hypothesis.

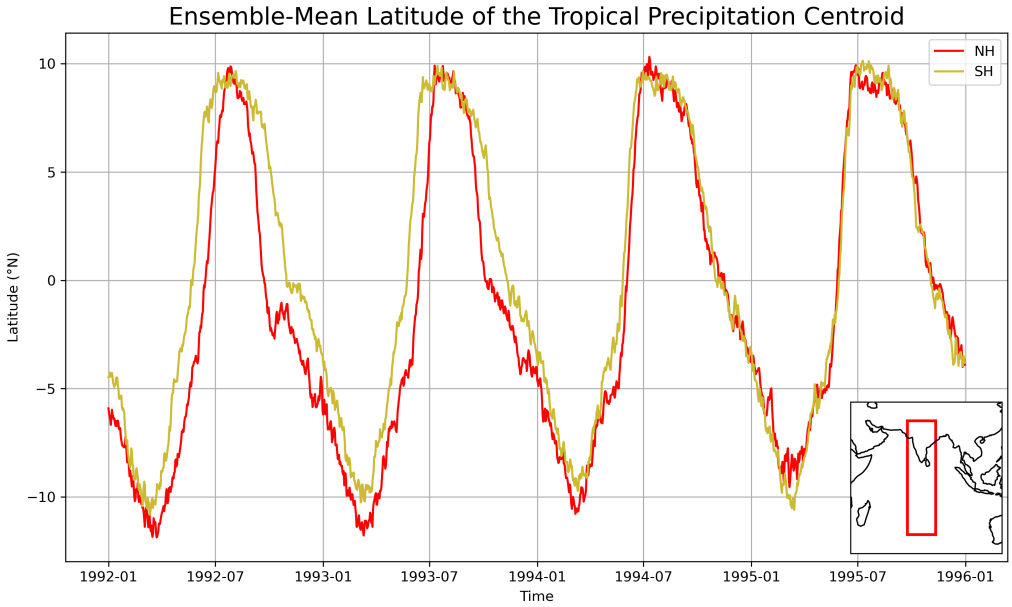

Figure 3.4: Movement of the latitude of the tropical (30 °S - 30 °N) precipitation centroid in the longitude band 70 - 85 °E (red rectangle in inset). The ensemble-mean latitude of the tropical precipitation centroids for the **NH** and **SH** experiments are compared.

Due to the antisymmetry of the volcanic forcings in the **NH** and **SH** experiments, we see a large difference in their relative TCZ positions. That the **SH** TCZ is North of the **NH** TCZ is consistent with an earlier onset and later demise of the monsoon in the **SH** experiment. This implies that the **SH**'s tropical circulation switches from the equinox to the monsoon pattern earlier and switches back from the monsoon pattern to the equinox pattern later.

We also note, however, that the difference in TCZ latitude between **NH** and **SH** is seasonally dependent. The smallest difference in their latitudes occurs in the peak ISM season when both TCZs reach their northernmost extent.

Although the TCZ framework provides a qualitatively consistent picture, the rainfall over India is not zonally symmetric, nor is it affected solely by inter-hemispheric temperature contrasts. Zonally asymmetric cooling and changes in pressure gradients also impact the monsoon, whose effects are analysed in the following section.

3.2.2 Low-Level-Jet Framework

Although a pressure gradient in the West of India, through the strengthening of the LLJ, has been used to explain the interannual variations in onset dates using observational data, it has not been used in the context of the volcanically forced response of monsoon onset. Within the LLJ framework, we would expect, given that there is a delayed onset in the **NH** and **TR** experiments, an anomalous high-pressure over the West of India, in the month of May. Similarly, we would expect an anomalous low in

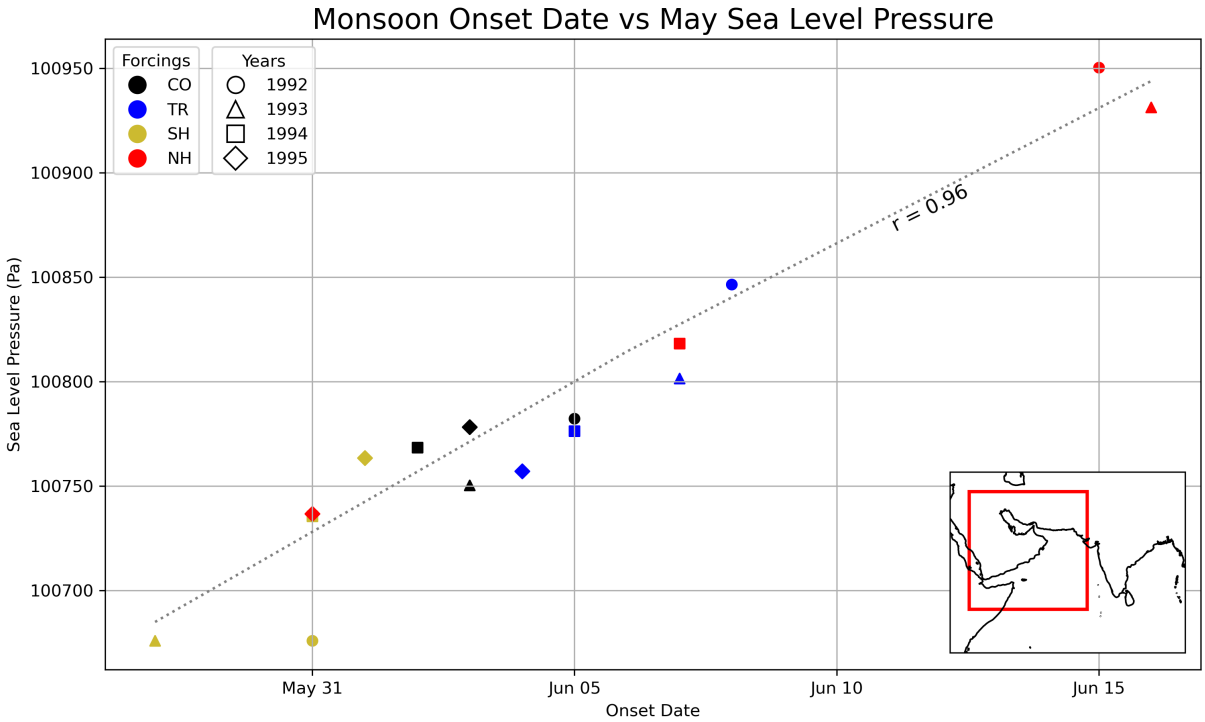

Figure 3.5: The ensemble-mean sea level pressure averaged over 40 - 70 °E, 5 - 30 °N (red rectangle in inset) in the month of May is regressed on the ensemble-mean onset date in all four experiments, for model years 1992 - 1995. The grey dotted line is the regression line of the ensemble-mean points.

the **SH** experiment.

This is indeed what is seen in Figure 3.5, where a very strong correlation exists between the onset date and the sea level pressure (SLP) West of India. It is then expected that the LLJ would be anomalously weak in the **NH** and **CO** experiments while being anomalously strong in the **SH** experiments. That is the case for the first two experiments, as seen in Figure 3.6 a) and b), which is in agreement with the results of Chakraborty and Agrawal [31]. We also find a delayed onset is correlated with weakened LLJ, seen in the Arabian Sea and Indian Ocean as the anomalous Easterly (Westerly) North (South) of the equator and an anomalous high pressure over this region. However, an anomalously strong jet over India is not seen in the **SH** experiment (Figure 3.6 c)), despite both an anomalously low SLP and early onset.

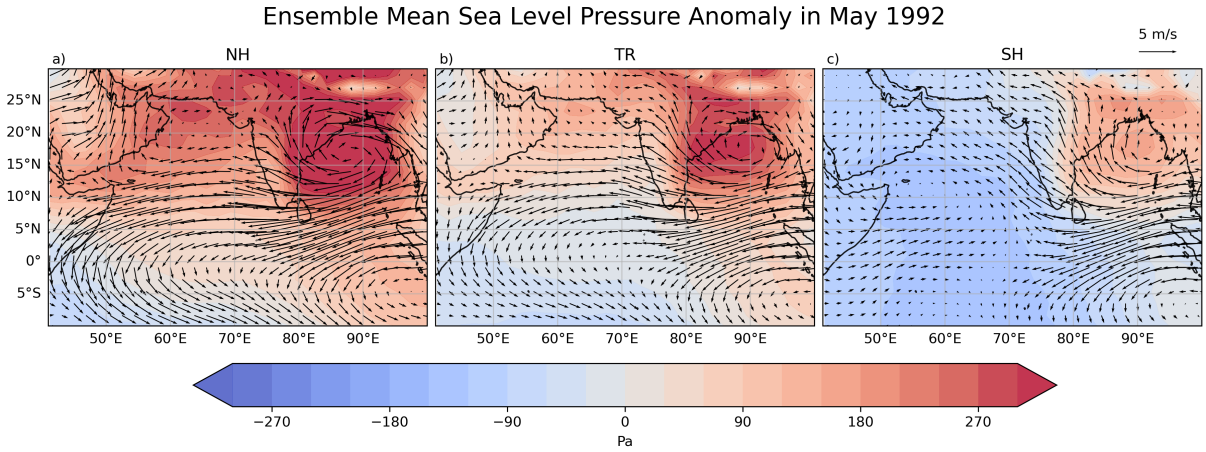

Figure 3.6: The anomalous ensemble-mean sea level pressure in May 1992. The anomalies are calculated for the ensemble-mean of the three forced experiments a) **TR**, b) **SH**, and c) **NH** with respect to the ensemble mean **CO**. The black arrows denote the ensemble-mean 850hPa horizontal wind velocity vector anomalies for the same.

However, as discussed in Section 1.2, the strengthening of the LLJ brings about the ISM onset through the convergence of winds and moisture. Therefore, a greater moisture convergence over India could be the cause of an earlier onset in the **SH** experiment despite a lack of relative strengthening of the LLJ. So, we look at the moisture convergence over central India in Figure 3.7.

We find, consistent with the prior knowledge of the LLJ, that large moisture convergence occurs in the days before onset. The **SH** experiment experiences an earlier 1992 onset despite not having a stronger LLJ in the month of May, due to the sudden increase in moisture convergence over India.

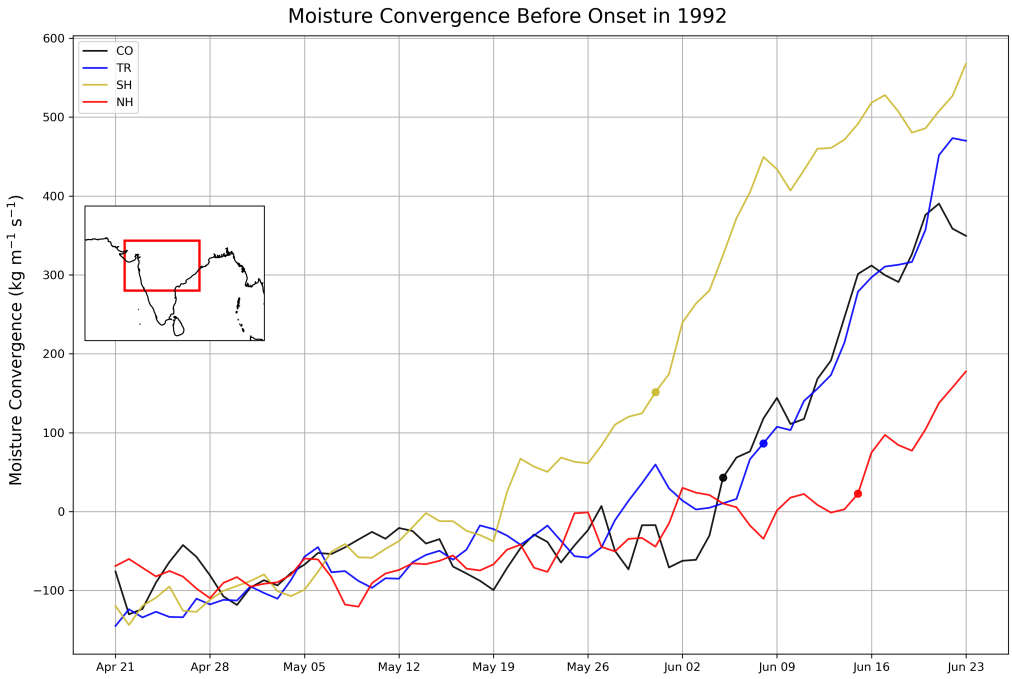

Figure 3.7: The ensemble-mean vertically integrated moisture flux into central India (red rectangle in the inset: $70 - 85$ °E, $15 - 25$ °N)) in 1992 for all four experiments. Dots mark the onset dates and corresponding moisture convergence.

While the timing of the increase in moisture convergence is consistent with the onset date of the ISM, the premonsoon anomaly in LLJ strength can only explain the delayed onset found in the **NH** and **TR** experiments.

Thus, the changes we find in the life cycle of the ISM can, at least qualitatively, be understood by the existing frameworks of the tropical convergence zone migration, as well as the moisture convergence over India. In the following subsection, we look at how the monsoon season precipitation is affected by changes in the seasonal length.

3.2.3 Monsoon Precipitation and Length

The precipitation-length relation of the ISM, seen in observational data (Section 1.2.1), is maintained in all the forced, as well as the **CO** experiments, as seen in Figure 3.8. We find that the multi-year IMD mean agrees with ensemble mean of the **CO** experiment on both the total monsoon precipitation and length. The large decrease found in monsoon precipitation in the **NH** experiment is accompanied by a decrease in length. This decrease lies largely on the same precipitation-length relation that holds for **CO**. This is also true for the **SH** experiment, but in the opposite direction as **NH**, with an increase in both precipitation and length. This shows that the dominant factor in changing the seasonal precipitation response of the ISM following a volcanic eruption is the length of the monsoon, contrary to the current understanding that the volcanically-

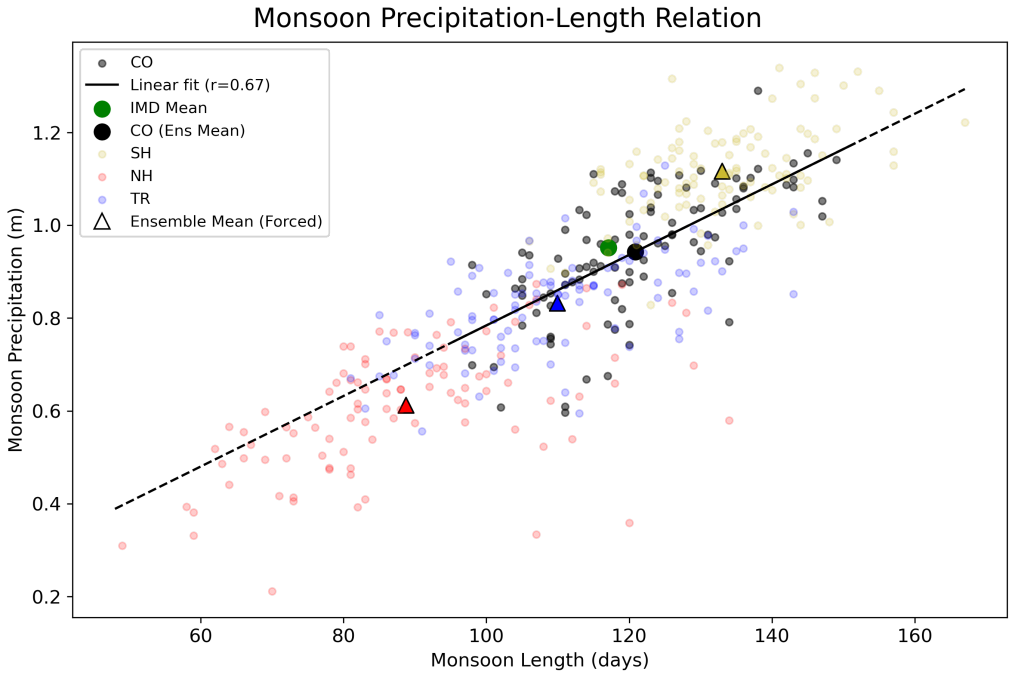

Figure 3.8: A scatter plot of the monsoon season precipitation and length for IMD's 1952-2024 data, and the 1992 model year for the four experiments, along with their ensemble mean. The linear regression of precipitation and length for the **CO** experiment is shown in the solid black curve and is extended to the width of the graph with the dashed line.

forced monsoon circulation strength is affected by changing land-sea contrasts.

However, the forced experiments also show some deviations from the precipitation-length axis. In the **NH** (**SH**) experiment, the ensemble mean precipitation is lower (higher) than expected for its seasonal length, if the precipitation-length relationship were to hold. Thus, the intensity of monsoon intensity of the **NH** (**SH**) is weaker (stronger) than the **CO** experiment. This deviation is consistent with a weaker **NH** circulation, and a stronger **SH** circulation. We also find that changes in **TR** experiment occur in the same direction as the **NH** experiment, but with a reduced magnitude.

Thus, we find that although the duration of the ISM is primarily responsible for determining the total ISM precipitation, deviations from this relation are in agreement with previous studies that attribute changes in ISM precipitation to a change in ISM circulation strength.

3.3 Discussion

Our results show significant changes in the ISM life cycle for a few years following volcanic eruptions. These changes persist for a duration comparable to the lifetime of stratospheric sulphur aerosols. However, certain geoengineering scenarios, such as stratospheric aerosol intervention (SAI), are designed to exert longer-term climatic

effects. SAI studies such as Simpson et al. [47] show a reduction in the JJA rainfall over India under SAI scenarios. We hypothesise that this reduction in monsoon intensity, similar to volcanic eruption scenarios, is also driven by a shorter ISM duration. In both SAI and volcanic eruption scenarios, the reduced ISM precipitation, combined with a delayed onset and earlier demise, would have adverse effects on Indian agriculture and its economy [48]. Moreover, since the onset of the ISM is accompanied by a reduction in the intensity of heatwaves, a delayed onset would lead to greater heat stress. However, due to the surface cooling effect of stratospheric aerosols, it is unclear which effect would dominate and whether SAI, contrary to its goal, would actually increase the summer heat stress over India.

Based on the large changes we find in ISM duration for different volcanic forcings, we believe the usage of a fixed climatological rainy season (such as JJAS) would be prone to contamination from the inclusion of dry season data. This would, even in the absence of any changes to the overall intensity of the monsoon, lead to a relative change in the average rainfall intensity over the fixed rainy season, as shown in previous studies. Although our results, in agreement with these previous studies, show an increase (decrease) in the monsoon season intensity in the **SH** (**NH**) experiment, we find its effect on the total ISM precipitation is secondary to those caused by changes in the monsoon season length.

In addition to volcanic eruptions directly impacting the monsoon life cycle, they also affect modes of internal variability, such as the El Nino Southern Oscillation (ENSO), leading to indirect effects on the monsoon. The response of the ENSO phase to volcanic eruptions has been studied (e.g. Stevenson et al. [49], Pausata et al. [35]), and so have the effects of ENSO on the ISM onset and precipitation (eg. Xavier et al. [50], Chakraborty and Singhai [51]). In order to disentangle the ENSO-mediated effects on the ISM from direct volcanic effects, an approach involving prescribing the sea-surface temperature (SST) was considered. The absence of an ocean response to volcanic forcing would limit the influence of indirect volcanic effects on the ISM life cycle. However, this approach would fail to represent the ocean-atmosphere interactions leading to monsoon onset, such as the wind-evaporation-SST feedback that has been linked to the strengthening of the LLJ [52], which would result in a flawed representation of the ISM onset.

We find no strengthening of the LLJ in the **SH** experiment compared to **CO** in the premonsoon season, despite an earlier onset. In contrast, we find the **NH** and **TR** experiments do exhibit a weakened LLJ much before onset. The LLJ framework is thus only partially successful in explaining volcanically-forced shifts in the ISM date. A possible reason for this incomplete explanation could be that the aerosols in the **SH** experiment exert an indirect forcing, being confined to the Southern Hemisphere, while the **NH** and **TR** experiments directly force the ISM. Chakraborty et al. [53] showed in

a study of tropospheric black carbon aerosols that direct and indirect forcings on the ISM exert their influence using two different mechanisms. In this study, the effect of local and remote aerosol forcings was compared. Changes in ISM precipitation due to local forcings were attributed to changes in the premonsoon moist static stability of the atmosphere, which was associated with pre-monsoon heating, which in turn increased net moisture flux into this region. Changes in the ISM due to remote forcings, on the other hand, were attributed to changes in the Rossby waves at 200 hPa and lower tropospheric moisture, which remotely influence the ISM precipitation. Although these mechanisms explain changes in the ISM due to tropospheric low-albedo aerosols, whether these are also relevant to stratospheric high-albedo aerosols remains unclear.

In this thesis, we have focused on the Indian summer monsoon, which is just one of the many existing regional monsoons. In the context of the TCZ framework, we expect the response of the life-cycle of other monsoons to be qualitatively similar to the ISM, with the same (opposite)-hemisphere eruption shortening (lengthening) the monsoon season length. Since our methodology does not use any rigid thresholds in the definition of the monsoon onset and demise, it can be used, with a few modifications, to find and compare the response of all regional monsoons to volcanic forcings in our model.

However, even though models have been used extensively to understand the monsoon response to volcanic eruptions, they have some limitations:

- The MPI-ESM was run in a coarse-resolution configuration, with a horizontal resolution of 200 km, due to which the influence of orography, and orographic rainfall is greatly reduced, which are important to represent the monsoon [21]. Additionally, convection in the MPI-ESM is parametrised, limiting its ability to model convective rainfall.

- The experiments prescribe volcanic forcings with a strength of 40 Tg of S. Such large eruptions are exceedingly rare. However, smaller eruptions have a smaller climate impact, with their signal being harder to distinguish from internal variability, with model eruptions no larger than Pinatubo having tropical precipitation effects on the threshold of detectability [17].

- The simplicity of the EVA generator limits its ability to capture the volcanic effects on stratospheric dynamics. Moreover, its prescribed nature prevents the interaction of aerosols with changes in stratosphere dynamics. Zhuo et al. [14] find, using the MPI-ESM and EVA generator, that the climate response was insensitive to eruption season. However, the seasonality of eruptions is important in determining the stratospheric aerosol distribution, while we consider only the effects of boreal summer volcanic eruptions on the monsoon.

Chapter 4

Summary and Conclusions

In this thesis, we find, using large ensemble simulations of the MPI-ESM, that large volcanic eruptions shift the life cycle of the Indian summer monsoon for a few years. Northern hemispheric and tropical eruptions delay the onset and advance the demise of the ISM, leading to a shorter monsoon season. Conversely, Southern hemispheric eruptions advance the onset and delay the demise of the ISM, lengthening its duration. These changes, especially reductions in the ISM length, have profound implications for India's agricultural productivity, economy, and water resources.

The shifts in the ISM onset and demise are qualitatively consistent with the TCZ framework of the monsoon, wherein the TCZ is displaced away from the cooled hemisphere by hemispherically asymmetric forcings, affecting its Northward migration in the boreal summer.

A large increase in moisture convergence precedes the monsoon onset in all model experiments. However, the strength of the LLJ in the premonsoon month of May is associated with the timing of this rapid increase in moisture convergence only in the experiments with a delayed monsoon onset (**NH** and **TR**). We find in these two experiments that the delayed onset is preceded by an anomalously weak low-level jet and an increased surface pressure in the Arabian Sea region. These anomalies are seen multiple weeks before onset, consistent with the onset changes due to internal variability [31]. However, despite the earlier onset in the **SH** experiment, there is no anomalously strong low-level jet, indicating that the LLJ framework can only partially explain variations in volcanically forced onset.

Previous studies of the monsoon region have looked at volcanic forcings affecting the seasonal average rainfall of the monsoon region (eg. [9, 16, 17, 15]). They attribute changes in the seasonal mean rainfall to a change in the strength of the monsoon circulation driven by differential land-sea cooling. However, observational data has shown that the total monsoon rainfall is correlated with the seasonal length [23]. The usage of an average rainfall intensity over a fixed monsoon season fails to consider changes in the duration of the monsoon season and its effect on the total

monsoon rainfall. We show that the shift in Indian summer monsoon rainfall, caused by volcanic forcings, is driven predominantly by changes in the duration of the monsoon season and not, as previously thought, by changes in the intensity of the monsoon precipitation.

References

[1] Christian E. Junge, Charles W. Chagnon, and James E. Manson. STRATOSPHERIC AEROSOLS. *Journal of the Atmospheric Sciences*, 18(1):81–108, February 1961. ISSN 1520-0469. doi: 10.1175/1520-0469(1961)018<0081:SA>2.0.CO;2.

[2] Theodore G. Shepherd. Large-Scale Atmospheric Dynamics for Atmospheric Chemists. *Chemical Reviews*, 103(12):4509–4532, December 2003. ISSN 0009-2665. doi: 10.1021/cr020511z.

[3] Claudia Timmreck. *Climatic effects of large volcanic eruptions*. habilitation, Max-Planck-Institut für Meteorologie, Hamburg, 2018.

[4] Alan Robock. Volcanic eruptions and climate. *Reviews of Geophysics*, 38(2): 191–219, May 2000. ISSN 8755-1209, 1944-9208. doi: 10.1029/1998RG000054.

[5] Paul A. O'Gorman, Richard P. Allan, Michael P. Byrne, and Michael Previdi. Energetic Constraints on Precipitation Under Climate Change. *Surveys in Geophysics*, 33(3):585–608, July 2012. ISSN 1573-0956. doi: 10.1007/s10712-011-9159-6.

[6] G. Bala, P. B. Duffy, and K. E. Taylor. Impact of geoengineering schemes on the global hydrological cycle. *Proceedings of the National Academy of Sciences*, 105 (22):7664–7669, June 2008. doi: 10.1073/pnas.0711648105.

[7] Anthony J. Broccoli, Keith W. Dixon, Thomas L. Delworth, Thomas R. Knutson, Ronald J. Stouffer, and Fanrong Zeng. Twentieth-century temperature and precipitation trends in ensemble climate simulations including natural and anthropogenic forcing. *Journal of Geophysical Research: Atmospheres*, 108(D24), 2003. ISSN 2156-2202. doi: 10.1029/2003JD003812.

[8] Alan Robock and Yuhe Liu. The Volcanic Signal in Goddard Institute for Space Studies Three-Dimensional Model Simulations. *Journal of Climate*, 7(1):44–55, January 1994. ISSN 0894-8755, 1520-0442. doi: 10.1175/1520-0442(1994)007<0044:TVSIGI>2.0.CO;2.

[9] David P. Schneider, Caspar M. Ammann, Bette L. Otto-Bliesner, and Darrell S. Kaufman. Climate response to large, high-latitude and low-latitude volcanic eruptions in the Community Climate System Model. *Journal of Geophysical Research: Atmospheres*, 114(D15), 2009. ISSN 2156-2202. doi: 10.1029/2008JD011222.

[10] Anthony J. Broccoli, Kristina A. Dahl, and Ronald J. Stouffer. Response of the ITCZ to Northern Hemisphere cooling. *Geophysical Research Letters*, 33(1): 2005GL024546, January 2006. ISSN 0094-8276, 1944-8007. doi: 10.1029/2005GL024546.

[11] Sarah M. Kang, Isaac M. Held, Dargan M. W. Frierson, and Ming Zhao. The response of the ITCZ to extratropical thermal forcing: Idealized slab-ocean experiments with a GCM. *Journal of Climate*, 21(14):3521–3532, July 2008. ISSN 0894-8755. doi: 10.1175/2007JCLI2146.1.

[12] Jim M. Haywood, Andy Jones, Nicolas Bellouin, and David Stephenson. Asymmetric forcing from stratospheric aerosols impacts Sahelian rainfall. *Nature Climate Change*, 3(7):660–665, July 2013. ISSN 1758-6798. doi: 10.1038/nclimate1857.

[13] Zhihong Zhuo, Chaochao Gao, and Yuqing Pan. Proxy evidence for China's monsoon precipitation response to volcanic aerosols over the past seven centuries. *Journal of Geophysical Research: Atmospheres*, 119(11):6638–6652, 2014. ISSN 2169-8996. doi: 10.1002/2013JD021061.

[14] Zhihong Zhuo, Ingo Kirchner, Stephan Pfahl, and Ulrich Cubasch. Climate impact of volcanic eruptions: The sensitivity to eruption season and latitude in MPI-ESM ensemble experiments. *Atmospheric Chemistry and Physics*, 21(17):13425–13442, September 2021. ISSN 1680-7324. doi: 10.5194/acp-21-13425-2021.

[15] Fei Liu, Jing Chai, Bin Wang, Jian Liu, Xiao Zhang, and Zhiyuan Wang. Global monsoon precipitation responses to large volcanic eruptions. *Scientific Reports*, 6(1):24331, April 2016. ISSN 2045-2322. doi: 10.1038/srep24331.

[16] Meng Zuo, Tianjun Zhou, and Wenmin Man. Hydroclimate Responses over Global Monsoon Regions Following Volcanic Eruptions at Different Latitudes. *Journal of Climate*, 32(14):4367–4385, July 2019. ISSN 0894-8755, 1520-0442. doi: 10.1175/JCLI-D-18-0707.1.

[17] Roberta D'Agostino and Claudia Timmreck. Sensitivity of regional monsoons to idealised equatorial volcanic eruption of different sulfur emission strengths. *Environmental Research Letters*, 17(5):054001, May 2022. ISSN 1748-9326. doi: 10.1088/1748-9326/ac62af.

[18] Ernesto Tejedor, Nathan J. Steiger, Jason E. Smerdon, Roberto Serrano-Notivoli, and Mathias Vuille. Global hydroclimatic response to tropical volcanic eruptions over the last millennium. *Proceedings of the National Academy of Sciences*, 118 (12):e2019145118, March 2021. doi: 10.1073/pnas.2019145118.

[19] K. J. Anchukaitis, B. M. Buckley, E. R. Cook, B. I. Cook, R. D. D'Arrigo, and C. M. Ammann. Influence of volcanic eruptions on the climate of the Asian monsoon region. *Geophysical Research Letters*, 37(22), 2010. ISSN 1944-8007. doi: 10.1029/2010GL044843.

[20] Pin Xian Wang, Bin Wang, Hai Cheng, John Fasullo, ZhengTang Guo, Thorsten Kiefer, and ZhengYu Liu. The global monsoon across time scales: Mechanisms and outstanding issues. *Earth-Science Reviews*, 174:84–121, November 2017. ISSN 0012-8252. doi: 10.1016/j.earscirev.2017.07.006.

[21] A. Chakraborty, R. S. Nanjundiah, and J. Srinivasan. Theoretical aspects of the onset of Indian summer monsoon from perturbed orography simulations in a GCM. *Annales Geophysicae*, 24(8):2075–2089, September 2006. ISSN 1432-0576. doi: 10.5194/angeo-24-2075-2006.

[22] B. N. Goswami and R. S. Ajaya Mohan. Intraseasonal Oscillations and Interannual Variability of the Indian Summer Monsoon. *Journal of Climate*, 14(6):1180–1198, March 2001. ISSN 0894-8755, 1520-0442. doi: 10.1175/1520-0442(2001)014<1180:IOAIVO>2.0.CO;2.

[23] Ryne Noska and Vasubandhu Misra. Characterizing the onset and demise of the Indian summer monsoon. *Geophysical Research Letters*, 43(9):4547–4554, May 2016. ISSN 0094-8276, 1944-8007. doi: 10.1002/2016GL068409.

[24] Rumi Aijaz. Monsoon Variability and Agricultural Drought Management in India. https://www.orfonline.org/research/monsoon-variability-and-agricultural-drought-management-in-india, May 2013.

[25] Sulochana Gadgil and K. Rupa Kumar. The Asian monsoon — agriculture and economy. In Bin Wang, editor, *The Asian Monsoon*, pages 651–683. Springer, Berlin, Heidelberg, 2006. ISBN 978-3-540-37722-1. doi: 10.1007/3-540-37722-0_18.

[26] Sulochana Gadgil. The Indian Monsoon and Its Variability. *Annual Review of Earth and Planetary Sciences*, 31(1):429–467, May 2003. ISSN 0084-6597, 1545-4495. doi: 10.1146/annurev.earth.31.100901.141251.

[27] Simona Bordoni and Tapio Schneider. Monsoons as eddy-mediated regime transitions of the tropical overturning circulation. *Nature Geoscience*, 1(8):515–519, August 2008. ISSN 1752-0894, 1752-0908. doi: 10.1038/ngeo248.

[28] Massimo Bollasina and Sumant Nigam. The summertime "heat" low over Pakistan/northwestern India: Evolution and origin. *Climate Dynamics*, 37(5):957–970, September 2011. ISSN 1432-0894. doi: 10.1007/s00382-010-0879-y.

[29] J. Findlater. A major low-level air current near the Indian Ocean during the northern summer. *Quarterly Journal of the Royal Meteorological Society*, 95(404): 362–380, 1969. ISSN 1477-870X. doi: 10.1002/qj.49709540409.

[30] David Halpern and Peter M. Woiceshyn. Onset of the Somali Jet in the Arabian Sea during June 1997. *Journal of Geophysical Research: Oceans*, 104(C8): 18041–18046, 1999. ISSN 2156-2202. doi: 10.1029/1999JC900141.

[31] Arindam Chakraborty and Shubhi Agrawal. Role of west Asian surface pressure in summer monsoon onset over central India. *Environmental Research Letters*, 12(7):074002, July 2017. ISSN 1748-9326. doi: 10.1088/1748-9326/aa76ca.

[32] Rodrigo J. Bombardi, Vincent Moron, and James S. Goodnight. Detection, variability, and predictability of monsoon onset and withdrawal dates: A review. *International Journal of Climatology*, 40(2):641–667, February 2020. ISSN 0899-8418, 1097-0088. doi: 10.1002/joc.6264.

[33] T. J. Crowley and M. B. Unterman. Technical details concerning development of a 1200 yr proxy index for global volcanism. *Earth System Science Data*, 5(1): 187–197, May 2013. ISSN 1866-3508. doi: 10.5194/essd-5-187-2013.

[34] Sebastian Milinski, Nicola Maher, and Dirk Olonscheck. How large does a large ensemble need to be? *Earth System Dynamics*, 11(4):885–901, October 2020. ISSN 2190-4979. doi: 10.5194/esd-11-885-2020.

[35] Francesco S. R. Pausata, Davide Zanchettin, Christina Karamperidou, Rodrigo Caballero, and David S. Battisti. ITCZ shift and extratropical teleconnections drive ENSO response to volcanic eruptions. *Science Advances*, 6(23):eaaz5006, June 2020. doi: 10.1126/sciadv.aaz5006.

[36] Alon Azoulay, Hauke Schmidt, and Claudia Timmreck. The Arctic Polar Vortex Response to Volcanic Forcing of Different Strengths. *Journal of Geophysical Research: Atmospheres*, 126(11):e2020JD034450, 2021. ISSN 2169-8996. doi: 10.1029/2020JD034450.

[37] Marco A. Giorgetta, Johann Jungclaus, Christian H. Reick, Stephanie Legutke, Jürgen Bader, Michael Böttinger, Victor Brovkin, Traute Crueger, Monika Esch, Kerstin Fieg, Ksenia Glushak, Veronika Gayler, Helmuth Haak, Heinz-Dieter Hollweg, Tatiana Ilyina, Stefan Kinne, Luis Kornblueh, Daniela Matei, Thorsten Mauritsen, Uwe Mikolajewicz, Wolfgang Mueller, Dirk Notz, Felix Pithan, Thomas Raddatz, Sebastian Rast, Rene Redler, Erich Roeckner, Hauke Schmidt, Reiner Schnur, Joachim Segschneider, Katharina D. Six, Martina Stockhause, Claudia Timmreck, Jörg Wegner, Heinrich Widmann, Karl-H. Wieners, Martin Claussen, Jochem Marotzke, and Bjorn Stevens. Climate and carbon cycle changes from 1850 to 2100 in MPI-ESM simulations for the Coupled Model Intercomparison Project phase 5. *Journal of Advances in Modeling Earth Systems*, 5(3):572–597, 2013. ISSN 1942-2466. doi: 10.1002/jame.20038.

[38] Nicola Maher, Sebastian Milinski, Laura Suarez-Gutierrez, Michael Botzet, Mikhail Dobrynin, Luis Kornblueh, Jürgen Kröger, Yohei Takano, Rohit Ghosh, Christopher Hedemann, Chao Li, Hongmei Li, Elisa Manzini, Dirk Notz, Dian Putrasahan, Lena Boysen, Martin Claussen, Tatiana Ilyina, Dirk Olonscheck, Thomas Raddatz, Bjorn Stevens, and Jochem Marotzke. The Max Planck Institute Grand Ensemble: Enabling the Exploration of Climate System Variability. *Journal of Advances in Modeling Earth Systems*, 11(7):2050–2069, 2019. ISSN 1942-2466. doi: 10.1029/2019MS001639.

[39] Bjorn Stevens, Marco Giorgetta, Monika Esch, Thorsten Mauritsen, Traute Crueger, Sebastian Rast, Marc Salzmann, Hauke Schmidt, Jürgen Bader, Karoline Block, Renate Brokopf, Irina Fast, Stefan Kinne, Luis Kornblueh, Ulrike Lohmann, Robert Pincus, Thomas Reichler, and Erich Roeckner. Atmospheric component of the MPI-M Earth System Model: ECHAM6. *Journal of Advances in Modeling Earth Systems*, 5(2):146–172, 2013. ISSN 1942-2466. doi: 10.1002/jame.20015.

[40] J. H. Jungclaus, N. Fischer, H. Haak, K. Lohmann, J. Marotzke, D. Matei, U. Mikolajewicz, D. Notz, and J. S. von Storch. Characteristics of the ocean simulations in the Max Planck Institute Ocean Model (MPIOM) the ocean component of the MPI-Earth system model. *Journal of Advances in Modeling Earth Systems*, 5(2): 422–446, 2013. ISSN 1942-2466. doi: 10.1002/jame.20023.

[41] Davide Zanchettin, Claudia Timmreck, Myriam Khodri, Anja Schmidt, Matthew Toohey, Manabu Abe, Slimane Bekki, Jason Cole, Shih-Wei Fang, Wuhu Feng, Gabriele Hegerl, Ben Johnson, Nicolas Lebas, Allegra N. LeGrande, Graham W. Mann, Lauren Marshall, Landon Rieger, Alan Robock, Sara Rubinetti, Kostas Tsigaridis, and Helen Weierbach. Effects of forcing differences and initial conditions

on inter-model agreement in the VolMIP volc-pinatubo-full experiment. *Geoscientific Model Development*, 15(5):2265–2292, March 2022. ISSN 1991-959X. doi: 10.5194/gmd-15-2265-2022.

[42] Matthew Toohey, Bjorn Stevens, Hauke Schmidt, and Claudia Timmreck. Easy Volcanic Aerosol (EVA v1.0): An idealized forcing generator for climate simulations. *Geoscientific Model Development*, 9(11):4049–4070, November 2016. ISSN 1991-9603. doi: 10.5194/gmd-9-4049-2016.

[43] M. Rajeevan, Jyoti Bhate, and A. K. Jaswal. Analysis of variability and trends of extreme rainfall events over India using 104 years of gridded daily rainfall data. *Geophysical Research Letters*, 35(18), 2008. ISSN 1944-8007. doi: 10.1029/2008GL035143.

[44] Saswata Nandi and Pratiman Patel. Iamsaswata/imdlib: A Python library for IMD gridded data. Zenodo, December 2020.

[45] Matthew Toohey and Michael Sigl. Volcanic stratospheric sulfur injections and aerosol optical depth from 500 BCE to 1900 CE. *Earth System Science Data*, 9 (2):809–831, November 2017. ISSN 1866-3508. doi: 10.5194/essd-9-809-2017.

[46] Vasubandhu Misra, Amit Bhardwaj, and Akhilesh Mishra. Local onset and demise of the Indian summer monsoon. *Climate Dynamics*, 51(5-6):1609–1622, September 2018. ISSN 0930-7575, 1432-0894. doi: 10.1007/s00382-017-3924-2.

[47] I. R. Simpson, S. Tilmes, J. H. Richter, B. Kravitz, D. G. MacMartin, M. J. Mills, J. T. Fasullo, and A. G. Pendergrass. The Regional Hydroclimate Response to Stratospheric Sulfate Geoengineering and the Role of Stratospheric Heating. *Journal of Geophysical Research: Atmospheres*, 124(23):12587–12616, 2019. ISSN 2169-8996. doi: 10.1029/2019JD031093.

[48] M. M. Nageswararao, Susmitha Joseph, Raju Mandal, Vijay Tallapragada, Javed Akhter, Avijit Dey, Rajib Chattopadhyay, R. Phani, and A. K. Sahai. The role of antecedent southwest summer monsoon rainfall on the occurrence of premonsoon heat waves over India in the present global warming era. *Discover Environment*, 2(1):127, November 2024. ISSN 2731-9431. doi: 10.1007/s44274-024-00166-7.

[49] Samantha Stevenson, Bette Otto-Bliesner, John Fasullo, and Esther Brady. "El Niño Like" Hydroclimate Responses to Last Millennium Volcanic Eruptions. *Journal of Climate*, 29(8):2907–2921, April 2016. ISSN 0894-8755, 1520-0442. doi: 10.1175/JCLI-D-15-0239.1.

[50] Prince K. Xavier, Charline Marzin, and B. N. Goswami. An objective definition of the Indian summer monsoon season and a new perspective on the ENSO–monsoon relationship. *Quarterly Journal of the Royal Meteorological Society*, 133(624):749–764, 2007. ISSN 1477-870X. doi: $10.1002/\mathrm{qj}.45$.

[51] Arindam Chakraborty and Priyanshi Singhai. Asymmetric response of the Indian summer monsoon to positive and negative phases of major tropical climate patterns. *Scientific Reports*, 11(1):22561, November 2021. ISSN 2045-2322. doi: $10.1038/\mathrm{s41598\text{-}021\text{-}01758\text{-}6}$.

[52] William R. Boos and Kerry A. Emanuel. Annual intensification of the Somali jet in a quasi-equilibrium framework: Observational composites. *Quarterly Journal of the Royal Meteorological Society*, 135(639):319–335, January 2009. ISSN 0035-9009, 1477-870X. doi: $10.1002/\mathrm{qj}.388$.

[53] Arindam Chakraborty, Ravi S. Nanjundiah, and J. Srinivasan. Local and remote impacts of direct aerosol forcing on Asian monsoon. *International Journal of Climatology*, 34(6):2108–2121, May 2014. ISSN 0899-8418, 1097-0088. doi: $10.1002/\mathrm{joc}.3826$.